SCIENTIFIC REPORTS

OPEN

SUBJECT AREAS:
PALAEOCLIMATE
PALAEOCEANOGRAPHY

Received
3 January 2014

Accepted
16 May 2014

Published
13 June 2014

Correspondence and requests for materials should be addressed to Y.T.H. (hongyetang@vip.skleg.cn)

Increasing summer rainfall in arid eastern-Central Asia over the past 8500 years

Bing Hong[1], Françoise Gasse[2], Masao Uchida[3], Yetang Hong[1], Xuetian Leng[4], Yasuyuki Shibata[3], Ning An[1], Yongxuan Zhu[1] & Yu Wang[1]

[1]State Key Laboratory of Environmental Geochemistry, Institute of Geochemistry, Chinese Academy of Sciences, 46 Guanshui Road, Guiyang, Guizhou 550002, China, [2]CEREGE, B.P.80, 13545, Aix-en-Provence Cedex 04, France, [3]Center for Environmental measurement and analysis, National Institute for Environmental Studies, Onogawa 16-2, Tsukuba, Ibaraki, 305-0053 Japan, [4]Institute of Peatmire, Northeast Normal University, Changchun, Jilin 130024, China.

A detailed and well-dated proxy record of summer rainfall variation in arid Central Asia is lacking. Here, we report a long-term, high resolution record of summer rainfall extracted from a peat bog in arid eastern-Central Asia (AECA). The record indicates a slowly but steadily increasing trend of summer rainfall in the AECA over the past 8500 years. On this long-term trend are superimposed several abrupt increases in rainfall on millennial timescales that correspond to rapid cooling events in the North Atlantic. During the last millennium, the hydrological climate pattern of the AECA underwent a major change. The rainfall in the past century has reached its highest level over the 8500-year history, highlighting the significant impact of the human-induced greenhouse effect on the hydrological climate in the AECA. Our results demonstrate that even in very dry eastern-Central Asia, the climate can become wetter under global warming.

Central Asia usually extends from the Caspian Sea in the west to the Daxinganling Mountains in the east between approximately 35°N and 55°N. The ancient channel for trade and cultural exchanges among Europe, Central Asia, and East Asia, namely the Silk Road, passes across the Central Asian region. The region of the AECA east of the Pamirs Plateau, which is one of the most arid areas in the world[1], consists of a distribution of widespread desert, loess, and sandy land (Fig. 1). It has been considered that the summer precipitation of the AECA is affected by the westerlies, the Indian summer monsoon (ISM), and the East Asian summer monsoon (EASM)[1–7]. This complex pattern of climate dynamics has stimulated the pursuit of sensitive and highly resolvable climate proxies that can provide clues about the primary physical processes affecting local wet and dry changes. Until recently, too few AECA summer rainfall records were available to establish whether summer precipitation operating at different timescales is tied to a certain physical process.

Here, we present a high resolution proxy record of palaeo-summer rainfall from the peat cellulose $\delta^{13}C$ of the Chaiwobu peatland in Xinjiang, China. The peatland, with an area of 3300 hm^2, grows in the Chaiwobu basin approximately 45 km southeast of Urumqi city, Xinjiang (Fig. 1). Geologically, the basin region belongs in the syncline fold belt of the north Tianshan Mountains. In the central part of the basin, there is a lowland that distributes in a northwest-southeast direction and is covered with alluvial-pluvial sediments more than 200 meters deep (Fig. 2 and Fig. S1). The annual average temperature is approximately 6.5°C, and the annual mean rainfall is approximately 250 mm in the lowland region. However, the mountain area surrounding the lowland receives plenty of rainfall. The annual mean rainfall reaches approximately 400–800 mm, with over 65% of the rainfall occurring in spring and summer[8] (Table 1 and Fig. S2). The water chemistry study suggests that the rainwater from the mountain area flows into the lowland or seeps into the ground through the piedmont alluvial fan and becomes the main source of groundwater in the central part of the basin[9]. The water table of the lowland is shallow, and spring water often flows out through the surface. These geological and climatic characteristics lead to the relatively wet surface soil of the lowland, the growth of meadow vegetation, the formation of the peat bog in the lowland region, and the sensitive response of the lowland environment to the climate change.

Previous research demonstrated that the $\delta^{13}C$ value of peat plant cellulose is a sensitive indicator of summer rainfall variability (see the detailed discussion in the following Methods section). In this study, the Chaiwobu peat cellulose $\delta^{13}C$ record is used for comparison with previously published records of the westerlies, the Asian monsoons, and atmospheric CO_2 concentrations to identify the primary physical processes affecting summer rainfall in

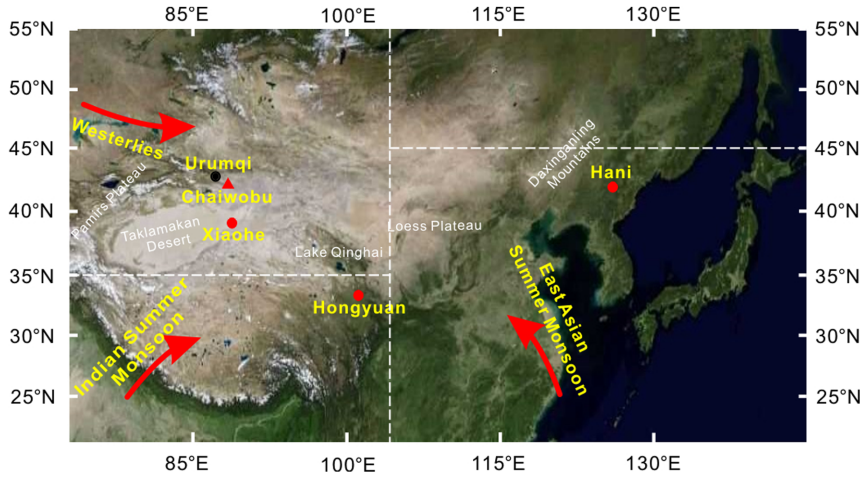

Figure 1 | Sketched map showing the location of the Chaiwobu peatland (red solid triangle) and some of the related research sites (red solid circles). The three boxed regions in the Chinese mainland and its adjacent areas define major summer precipitation areas: the westerly region (35–55°N, 50–105°E), the EASM region (22.5–45°N, 105–145°E), and the ISM region (5–35°N, 65–105°E). The base map was obtained from TIANDITU Co., LTD, China (GS, No.6034, 2013), and the related research marks were added using the CorelDRAW Graphics Suite 12.

the AECA. The results have important implications for understanding hydrological climate variability in the AECA in the current warming climate as well as for predicting trends in climate variability.

Results

Long-term trend of increasing summer rainfall. Currently, the climate divisions of the East Asian continent are still unrefined. Based on the seasonal fields of the modern monsoon stream function, air pressure, humidity, and precipitation, the Chinese mainland and its adjacent areas were divided into several different climate regions[10]. Subsequently, a more practical climate division presented by Wang et al. has been widely used in palaeoclimatology[11]. In this study, three regional boxes on the Chinese mainland and its adjacent areas are applied to define major summer precipitation areas according to the above mentioned climate divisions: the westerly region (35–55°N, 50–105°E), the EASM region (22.5–45°N, 105–145°E), and the ISM region (5–35°N, 65–105°E) (Fig. 1). The studied Chaiwobu region of Xinjiang is in the westerly region.

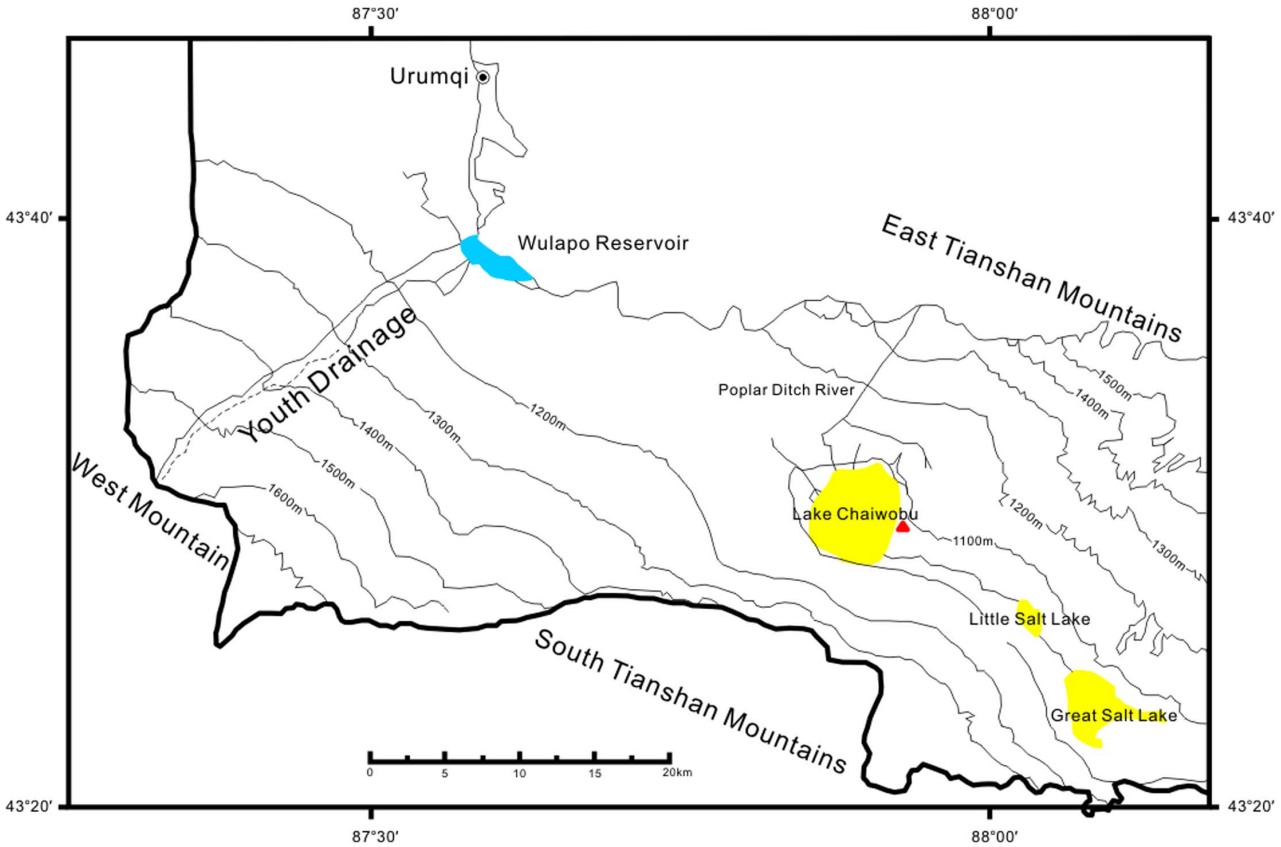

Figure 2 | Sketched map showing the topography of the Chaiwobu basin, Xinjiang. Thin lines with numbers are the terrain contours. The red triangle denotes the sampling location of the studied peat profile (modified from Yin X.L. et al.[9]).

Table 1 | Percentage of the Seasonal rainfall in annual precipitation in the different regions of Xinjiang, China during 1951 to 1980 (%)[8]

	Altay	Tacheng	Ili	Urumqi	Xiaoquzi	Qitai	Kumul	Turpan	Korla	Aksu	Kashgar	Hotan	Ruoqiang
Spring	21	29	31	33	29	27	18	14	18	19	36	31	17
Summer	29	27	25	30	50	37	50	52	62	60	32	42	62
Autumn	26	25	22	25	17	27	19	15	14	13	14	12	6
Winter	24	20	22	12	4	10	13	19	6	8	18	15	14

Summer rainfall in the westerly region is generally thought to result from the transport of moisture by the westerly wind. As research progresses, the understanding of the climate dynamics in the westerly area has gradually deepened. A competitive relationship between the growth and decline of the westerlies and the Asian monsoon has been gradually stressed. Currently, there is a debate focused on the dominant mechanism of climate variability in northwestern China: the westerlies or the EASM. Based on the study of vegetation and palynology, some researchers have suggested that the northern boundary of the Asian monsoon has moved over geological history and that during the last deglaciation and early-mid Holocene, the monsoon region covered the entire northern Chinese mainland, including northwestern China [Fig. 103 (d) of reference 2; Fig. 1 of reference 12]. Considering the high water level of most lakes in northern and central Mongolia during the mid-Holocene, some scientists have also suggested that the moisture-bearing summer monsoon may have extended its influence westward to Xinjiang and northward to northern Mongolia[1,3–5,13,14]. In contrast, others have shown that on the orbital timescale, the arid central Asia region that is dominated by westerlies experienced synchronous and coherent moisture changes during the Holocene and that the effective moisture history in central Asia is out of phase with that in monsoonal Asia[15]. This result implies that the monsoon barely extended to central Asia during the Holocene[15–17]. These arguments suggest the need for the development of a more sensitive, high resolution proxy climate record and the execution out more in-depth comparison and modelling studies.

Figure 3c shows that the $\delta^{13}C$ value of Chaiwobu peat cellulose continually decreased from approximately −24‰ to −27‰ over the last 8500 years, indicating an overall increasing trend of summer rainfall with some fluctuations (i.e., the climate in the AECA has become gradually wetter over that period). The decreasing trend of the peat $\delta^{13}C$ has a minor relationship to the variation of the $\delta^{13}C$ value of atmospheric CO_2 because the $\delta^{13}C$ of atmospheric CO_2 varied only from approximately −6.4‰ to −6.8‰[18,19] during the same period, which is insufficient to cause such a large variation in the peat $\delta^{13}C$ value. The gradual moistening of the climate is unlikely the result of increased water vapour content of the westerlies based on Fig. 3f, which shows that the strength of the westerlies climate index in the AECA remained stable during the period[7]. During this same period, the strength of the ISM gradually decreased[20–22] (Fig. 3e). Only the EASM strength, as inferred from the $\delta^{13}C$ of the Hani peat (42°13′N, 126°31′E), exhibited a similar increasing trend[23] (Fig. 3d). This correlation suggests that the increasing summer rainfall in the Chaiwobu region possibly results from the strengthening of the EASM transporting more water vapour to the northwestern Chinese mainland over the past 8500 years. This correlation also explains the results of a recent comprehensive study showing that the regionally averaged moisture index based on pollen and pollen-related moisture indicators in the Xinjiang region has been persistently climbing since approximately 10000 yr BP[24].

However, these findings do not mean that the effect of the westerlies can be neglected. In addition to the consideration of the water vapour content, verification of the effect of the westerlies from a kinetic perspective is also important. Based on the global reanalysis data sets provided by NCEP/NCAR, it is generally thought that in the background climate (or normal climatological conditions), the summer water vapour over the Chinese mainland originates mainly from ISA and EASM transport. The water vapour transport by the mid-latitude westerlies is relatively weak. In addition, the water vapour from the westerlies is mainly found in the upper atmosphere (approximately 500 hPa and above), whereas the monsoon moisture that greatly affects precipitation is mainly concentrated in the lower atmosphere (800 hPa and below)[25,26]. However, in the summer season the importance of the westerly, as a cold and dry air flow, is demonstrated when it encounters warm and humid monsoon water vapor that eventually results in the strong convergence over the main rainbelts, providing a highly beneficial background for abundant rainfall[25]. These results highlight that a strengthened Asian monsoon and westerlies are the two indispensable factors of the kinetic process of precipitation. Their encounter and convergence in the atmosphere play a fundamental role in the occurrence of summer rainfall in northern China.

Increase in summer rainfall on the millennial timescale. The interplay between a strengthening EASM and westerlies may also occur on the millennial timescale. Fig. 3c shows several increases in the summer rainfall on the millennial timescale superimposed on the long-term trend. A prominent characteristic of these rainfall variations is shown by the teleconnection with the rapidly cooling climate in the high northern latitudes. Summer rainfall in the AECA increased corresponding to several ice-rafted debris (IRD) cooling events (or Bond cycles) in the North Atlantic[27], for example, corresponding to the IRD events 1, 2, 3, and 5. During those same periods, however, no clear variation of the strength of the westerlies was observed (Fig. 3f)[7]; instead, the ISM clearly decreased[20,21,28] and the EASM clearly increased as inferred from the $\delta^{13}C$ of the Hani peat[23] (see the variations traced by the grey bars in Fig. 3). Therefore, a wetting climate on the millennial timescale in the AECA may also result from the interplay between the strengthening EASM and the westerlies. When the abrupt IRD cooling events occurred in the North Atlantic[27] and North China[29] (Figs. 3a and 3b), the warm and moisture-bearing EASM extended northwestward to the AECA and encountered cold, dry westerlies, which eventually resulted in the strong convergence of the EASM and the westerlies, thus providing conditions highly conducive to abundant rainfall. These results provide further evidence for the previous speculation that the monsoon extended toward the AECA[1–6,13,14].

This may be the first time the teleconnection between precipitation variability in the AECA and IRD cooling events in the North Atlantic has been uncovered, but similar teleconnections in other areas of the world have been widely studied. Based on 30 papers published since 1995, a recent review study suggests that this teleconnections do not always behave linearly. Often, some proxy records show more abrupt variations corresponding to IRD events than others[30]. It is generally considered that this nonlinear correspondence results mainly from the large spatial and temporal variability of climate, and precipitation in particular. This review study also suggests, however, that the cycles 2 and 5 are the most referred to in the 30 papers[30]. In the case of the Chaiwobu peat record (approximately 8500-year long), the four IRD events in the corresponding six

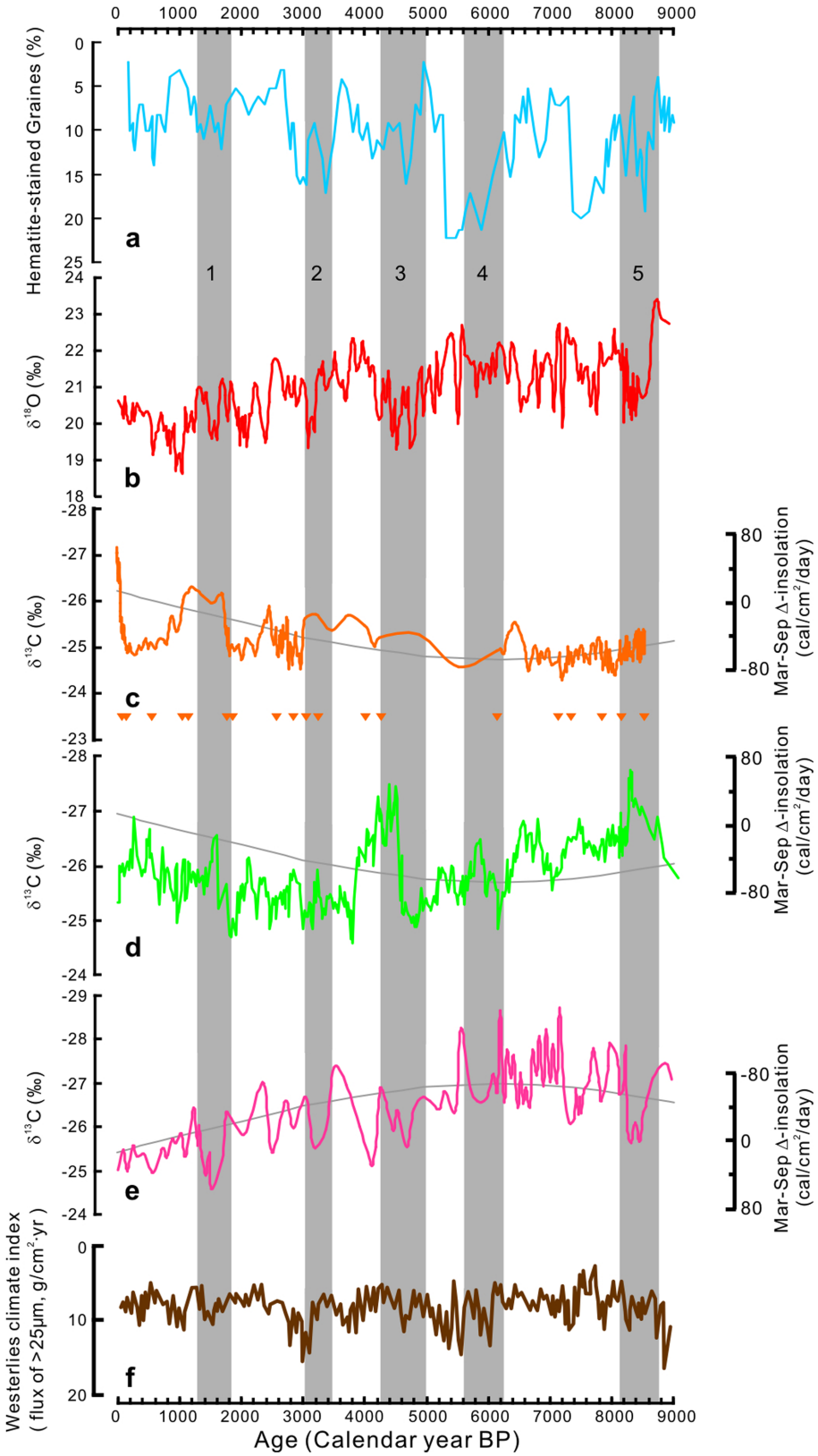

Figure 3 | The proxy record of summer rainfall in eastern-Central Asia inferred from $\delta^{13}C$ of Chaiwobu peat cellulose (c) and its comparison with related proxy climate records. The orange triangles show the calibrated ^{14}C age-control points of the Chaiwobu time series. (a) The drift ice record of the North Atlantic. The numbers from 1 to 5 indicate the five ice-rafted debris (IRD) events of the North Atlantic[27]. (b) The proxy temperature record from $\delta^{18}O$ of the Hani peat cellulose[29]. (d) The proxy record of the East Asian summer monsoon from $\delta^{13}C$ of the Hani peat cellulose[23]. (e) The proxy record of the Indian summer monsoon from $\delta^{13}C$ of the Hongyuan peat cellulose[21]. (f) The climate index of the westerlies from the flux of the >25 μm fraction in the Lake Qinghai sediments[7]. The grey curve shows the solar radiation difference between March and September at the equator as a measure of seasonality in the cold tongue of the eastern Equatorial Pacific[45]. The grey bars trace the teleconnection between the summer rainfall in eastern-Central Asia, the Asian monsoon, the westerlies, and the air temperature.

IRD events (0–5), including events 2 and 5, are recorded, showing that the Chaiwobu peat $\delta^{13}C$ record sensitively reflects the teleconnection between the local precipitation and the IRD cold event.

The AECA has not always been under severe drought conditions; on the contrary, the region is oscillating between wet and dry conditions on millennial timescales. An increase in precipitation that lasts for nearly one thousand years is clearly beneficial to drought mitigation and the improvement of eco-environmental quality. For example, responding to the abrupt strengthening of the EASM approximately 4500 yr BP (IRD event 3) (Fig. 3d)[23] and to the increase in summer rainfall in the AECA during the same period (Fig. 3c), evidence of the improved eco-environment in the AECA can be found through archaeology. In 2002, the extraordinary Xiaohe cemetery was excavated in the Taklamakan Desert, approximately 100 km south of the Chaiwobu peatland (Fig. 1). Based on the peculiar poplar markers at the Xiaohe cemetery, including 140 standing poles, wood coffins, and carved wooden statues with pronounced noses, archaeologists have suggested that the region once had lush poplar forests and that the local climate was wetter approximately 4000 years ago (uncalibrated radiocarbon (^{14}C) age)[31]. The wetter environment provided a suitable settlement area for a population migrating from the other areas, including Europe, and promoted the exchange of ancient cultures[31].

Rapid increases in summer rainfall over the last millennium. In recent years, the Chinese print media have reported an abnormal increase in summer rainfall in the Xinjiang area. Based on a comprehensive analysis of the modern meteorological and hydrological data, basic circulation patterns, and modelling studies, one hypothesis suggests that the precipitation in northwest China has clearly increased since 1987 AD and that the region's climate patterns have changed from warm-dry to warm-wet[4]. Our Chaiwobu record suggests that the start date of this wetting process was earlier than reported. In addition to a slowly and steadily increase in summer rainfall over the past 8500 years and superimposed abrupt increases in rainfall on millennial timescales, a rapid increase in summer rainfall started in approximately 1800 AD.

Figs. 3c and 4d show that the precipitation pattern of the AECA, inferred from the Chaiwobu peat $\delta^{13}C$, underwent a major change over the last millennium. Differing from the teleconnection with the IRD cooling event and from the slow and steady long-term increase, the summer rainfall of the AECA shows a more significant response to variations of atmospheric CO_2 concentration. The rainfall exhibited a change from slightly more to slightly less corresponding to the slightly higher levels of atmospheric CO_2 from approximately 1050–1200 AD (Medieval Climate Anomaly) and the slightly lower levels of CO_2 from1600–1750 AD (Little Ice Age) as recorded in Antarctic ice cores[32] (Figs. 4b and 4d). Since approximately 1800 AD, the atmospheric CO_2 concentration rapidly increased, which has generally been attributed to increasing anthropogenic impacts beginning with the industrial revolution[32], while the $\delta^{13}C$ value of atmospheric CO_2 exhibited only a small change from approximately −6.40‰ to −6.80‰ (Fig. 4a)[18]. Correspondingly, the $\delta^{13}C$ value of the Chaiwobu peat rapidly decreased. After deducting the impact of the Suess effect[33], the corrected curve of the peat $\delta^{13}C$ value still shows a sharp downward trend (Fig. 4d), indicating a dramatic increase in summer rainfall. Since start of the 20th century, the corrected $\delta^{13}C$ values have decreased to approximately −26.7‰, indicating the highest level of summer rainfall in the 8500-year history.

Some of the abnormal phenomena of climate change that occurred in northwest China over the past century are also recorded in the Chaiwobu peat. The record shows two significant fluctuations between approximately 1900 and 1950 AD (Fig. 4d). The peak ages of the two large $\delta^{13}C$ values are approximately 1910 and 1930 AD. It was this period from approximately 1920 to 1930 AD that the mean annual precipitation in north Xinjiang clearly decreased[34]. After many years of continuous precipitation deficit, an extreme drought occurred in northwest China from 1928 to 1929 AD. It caused two to three million deaths and caused low water levels on the Yellow River for 11 years from 1922 to 1932 AD[4]. According to the generally increasing trend of rainfall in the north Xinjiang region indicated by the modern meteorological and hydrological data[4], the generally decreasing trend of the corrected peat $\delta^{13}C$ value after 1950 AD may continue (Fig. 4d). This prediction is consistent with recent model predictions, that suggest large increases in wetness over Central and eastern Asia during the 21st century[35].

Discussion

The $\delta^{13}C$ record of the Chaiwobu peat has shown the precipitation history on three different timescales. The relationships between the summer rainfall and both the strengthening EASM on the millennial to orbital timescales and the atmospheric CO_2 concentration on the decadal to centennial timescales have also been described. However, the relevant dynamic mechanisms remain unclear and are still open for discussion.

In addition to the above mentioned impact of the westerlies, there are several factors that may influence precipitation in the AECA on millennial to orbital timescales. First, a cooling climate may act to inhibit evaporation and thus to increase the effective moisture. This means that decreasing air temperature on millennial to orbital timescales is one of the factors leading to wetter conditions in northwestern China. However, a cooling climate does not appear to be the primary reason because the climates of both northern and southern China cooled during the cooling episodes, i.e., the IRD events. Moreover, in recent years, the actual evaporative conditions in the arid and semi-arid areas of northern China have been re-estimated by applying newer standardized techniques to hydrological simulations and data from field observations. The results show that the loss of water in these areas was not as significant as previously believed and that the moisture variability in these areas was dominated by variations of monsoon intensity and precipitation[1]. Second, shifts in the mean latitude of the Intertropical Convergence Zone (ITCZ) are generally accompanied by significant changes in hydrological quantities in the tropics and subtropics. The dry climate in the ISM region during the middle and late Holocene is generally thought to be evidence of a southward migration of the ITCZ[30,36,37]. In our case, the phase relationship of the Asian monsoons may provide a more complete constraint for the hypothesis. The impact of ITCZ migration would be correct only when the variation of the precipitation in the ISM region is considered. It is difficult to explain why increasing EASM rainfall occurs in northern China or why the EASM strengthens after the southward shift of the ITCZ. It is clear that there should be other forcing factors in addition to the migration of the ITCZ. Third, the El Niño-Southern Oscillation (ENSO) phenomenon in the tropical Pacific Ocean may be one of the candidates. Many observational and modelling studies have suggested the close relationship between modern ENSO and monsoonal precipitation. In an El Niño year, the ISM rainfall tends to weaken[38–41] and the EASM rainfall tends to strengthen[42–44]. On the contrary, in a La Niña year, the ISM rainfall tends to strengthen and the EASM rainfall tends to weaken. A similar relationship seems to exist on the orbital timescale. By using the seasonality that is characterized by the equatorial insolation difference between March and September to indicate the influence of solar activity, one study has reported the relationship between sea surface temperature (SST) in the cold tongue of the eastern equatorial Pacific, the long-term ENSO pattern, and long-term solar activity[45,46]. In response to a gradual decline in seasonality during the period from approximately 8000–5000 yr BP, the SST in the cold tongue gradually decreased and the SST gradient in the equatorial Pacific was gradually enhanced, suggesting the presence of a long-term La Niña-like pattern in the equatorial Pacific during the period. In the late Holocene there has been mounting evidence for the occur-

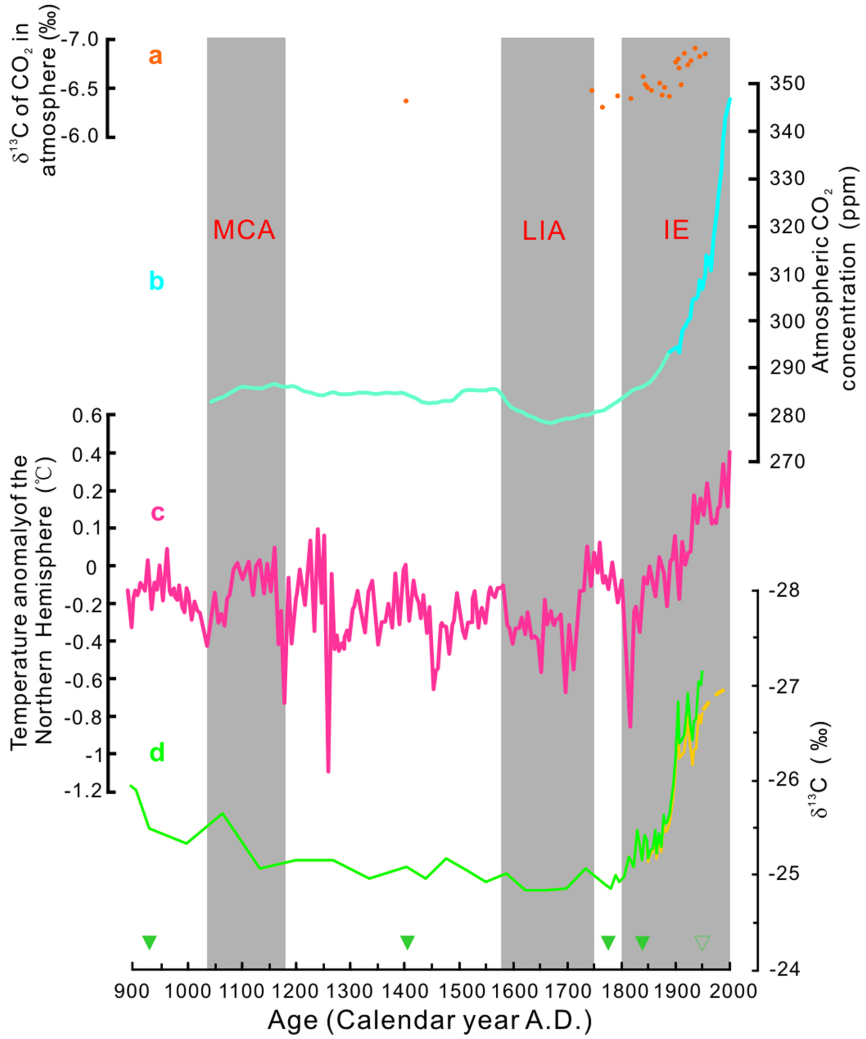

Figure 4 | A reconstruction of the summer rainfall history of eastern-Central Asia during the past millennium inferred from $\delta^{13}C$ of the Chaiwobu peat cellulose (green curve) (d) and its comparison with the related proxy climate records. The yellow curve is the corrected peat $\delta^{13}C$ curve between 1840 to 1950 AD after deducting the impact of the Suess effect using the method presented by Schelske C.L. et al.[33]. The dotted line indicates the predicted trend of summer rainfall according to the literature[4,35]. The green solid triangles denote the calibrated ^{14}C age-control points of the Chaiwobu time series (Table 2) and the green hollow triangle denotes the reference year for the calibrated ^{14}C age series that is 1950 AD. (a) $\delta^{13}C$ of the CO_2 in air extracted from an ice core from Siple Station in Antarctica[18]. (b) The CO_2 concentration in air extracted from ice cores in Antarctica, in which the light blue part of the CO_2 concentration data comes from WAIS Divide shallow core[32] and blue part of the CO_2 concentration data comes from the Siple Dome[18]. (c) Reconstruction of the mean temperature of the Northern Hemisphere[59]. The grey bars trace the correlations between the summer rainfall in eastern-Central Asia inferred from the Chaiwobu peat cellulose $\delta^{13}C$, $\delta^{13}C$ of atmospheric CO_2, atmospheric CO_2 concentration, and the mean temperature of the Northern Hemisphere. MCA refers to the Medieval Climate Anomaly. LIA refers to the Little Ice Age. IE refers to the industrial era.

rence of an El Niño-like pattern in the equatorial Pacific. It can be seen in Figs. 3d and 3e that corresponding to the long-term variations of seasonality and long-term ENSO activity, the two Asian monsoons show the inverse phase variations: the intensity of the EASM gradually changes from weak to strong, whereas the intensity of the ISM gradually changes from strong to weak[23]. The strength discrepancies of the two Asian monsoons on the orbital timescale have also been confirmed by modelling studies[47,48]. These comparisons show that the source of water vapour in the AECA on long timescales possibly has been primarily affected by the strengthening EASM. The impact of ENSO on the Asian monsoons also seems to exist on the millennial timescale and there seems to be a stronger relationship between the inverse phase variation of the Asian monsoon and an increase in ENSO frequency (Fig. 5). Fourth, Winkler and Wang drew the northern boundary of the Asian monsoon[2]. It is clear that this boundary is only an outline of the monsoon activity over a long timescale. More research is needed to understand the detailed spatial and temporal variations of the boundary.

As shown in Fig. 4, on the decadal to centennial timescale, there is a clear correspondence between variations in atmospheric CO_2 concentration, the Northern Hemisphere mean temperature, and the summer rainfall in the AECA. This correspondence highlights that the climate warming caused by the large amount of anthropogenic CO_2 possibly plays an important role in increasing summer rainfall in the AECA over the past 200 years, as it is generally accepted that the warming climate may change the global hydrological cycle[49]. The abruptly decreasing trend of the peat $\delta^{13}C$ value during the recent centuries is unlikely the result of local vegetation succession, since the Cyperaceae and Poaceae plants are the major components of the Chaiwobu peat and generally have the quite close $\delta^{13}C$ values. A similar phenomenon also occurred in geological history. During the Bølling-Allerød warming period, at approximately 14000 yr BP, the

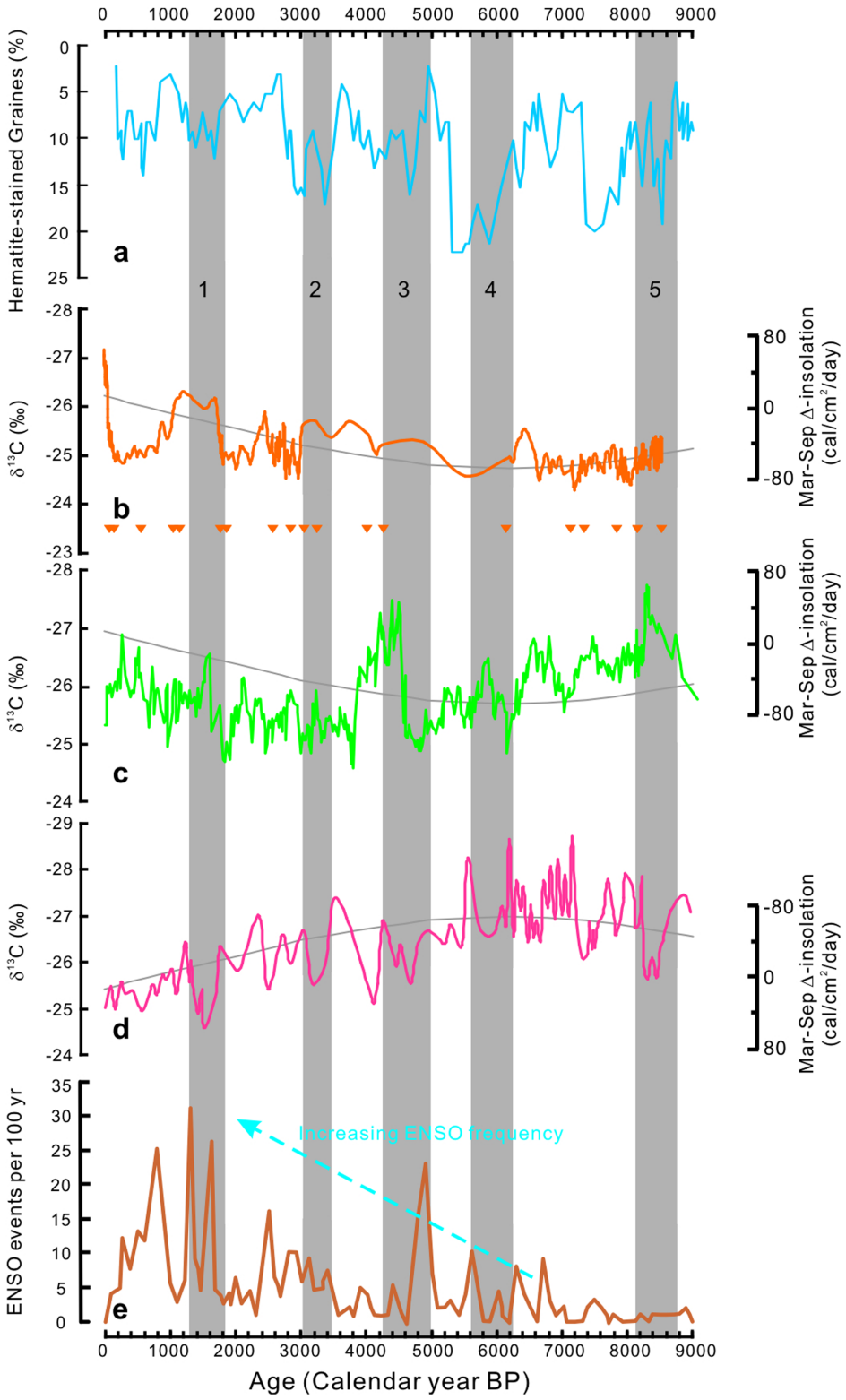

Figure 5 | The comparison of summer rainfall in eastern-Central Asia (b), the intensity of the East Asian summer monsoon[23] (c) and the Indian summer monsoon[21] (d), the climate variation of the high northern latitudes[27] (a), and the El Niño/Southern Oscillation (ENSO) frequency in the equatorial Pacific[60] (e). The grey bars trace the teleconnection among these variables on the millennial timescale. The orange triangles show the calibrated ^{14}C age-control points of the Chaiwobu time series. The numbers from 1 to 5 indicate the five ice-rafted debris (IRD) events of the North Atlantic[27]. The grey curve shows the solar radiation difference between March and September at the equator as a measure of seasonality in the cold tongue of the eastern Equatorial Pacific[45].

atmospheric CO_2 and CH_4 content was high[50], and the intensities of the two Asian monsoons were correspondingly strong[51–53]. However, there seems to be exception in geological history. It can be seen from Figs. 3c, 3d, 3e, and 3f that during the early-middle Holocene, the intensity of the EASM was weak, and the summer rainfall in the AECA was small, although the intensity of the ISM was strong during the same period, which has been attributed to the impact of ENSO-like patterns associated with long-term solar activity (as mentioned

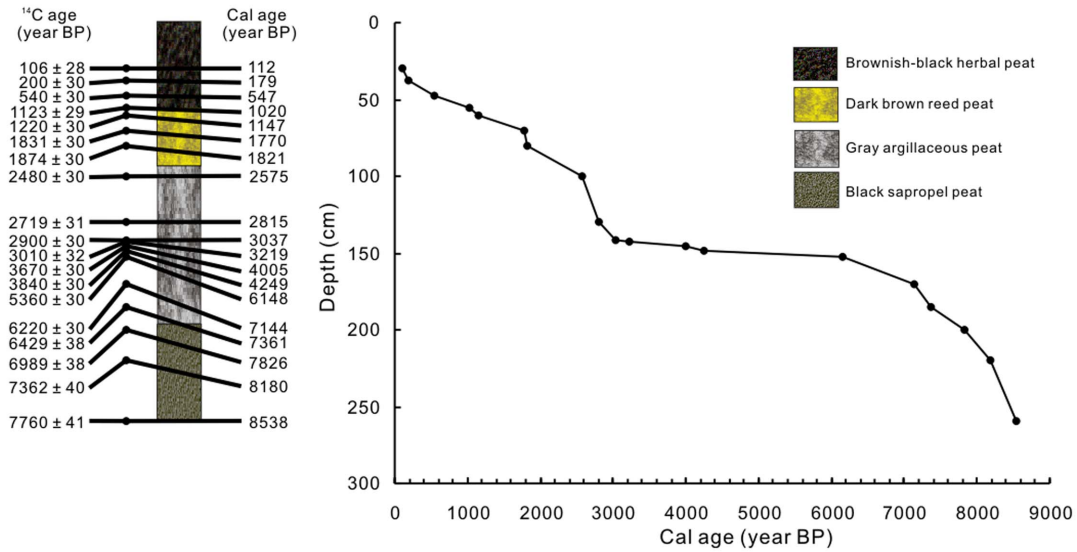

Figure 6 | Chronology and lithology of a fresh peat core from the Chaiwobu peat bog.

above). Therefore, whether the impacts of the increasing concentration of greenhouse gases and increased insolation on the hydrological cycle are equal remain unknown. If the concentration of greenhouse gases in the atmosphere, such as CO_2, CH_4, and N_2O, remain at high levels in the future, the AECA would welcome a historical opportunity to change to a wetter climate, balance the biogeochemical cycles of essential nutrients in drylands[54], and improve environmental quality. The establishment of a preventative system for sudden floods should also be considered because the local vegetation cover is currently very sparse.

Methods

Peat plant cellulose $\delta^{13}C$ value and summer rainfall. In the Chaiwobu peatland, an approximately 2.59 m-long peat core (43°29′N, 87°56′E, 1090 m above sea level) was obtained using a Russian peat corer and excavation. Identification of the peat core shows that the plant residues in the peat profile mainly consist of vascular Cyperaceae and Poaceae plants, such as *Carex enervis* C.A Mey., *Carex turkestanica* Rgl., *Eleocharis yokoseensis*, *Eriophorum vagihnatum* L., and *Phragmites australis* (Cav.) Trin. ex Steudel. Previous work has shown that the vascular sedge and grass families of C_3 plants exhibit a sensitive physiological response to the relative humidity of the growing environment by regulating the opening or closing of the leaf stomata. This activity leads to changes in the stable carbon isotopic composition of the atmospheric CO_2 utilised in plant photosynthesis[55,56]. Therefore, the variation of the $\delta^{13}C$ values of these herbaceous plants can sensitively reflect variations in relative humidity during their growing season. Relative humidity is defined as the ratio between the water vapour contained in the air and the saturation vapour amount at the given temperature. The larger the relative humidity is, the greater the water vapour content in the air at a given temperature. Once the monsoon stream containing warm water vapour meets cold air, such as the cold and dry westerlies, the air temperature will decrease, which will lead to a decrease in the saturation vapour, the condensation of the vapour, and eventually to the occurrence of rainfall. Therefore, in general, a large value of relative humidity indicates a high possibility of precipitation or a wetter climate, making relative humidity a good indicator of the precipitation variability. However, because the main growing season of the herbaceous plants in the research area is the late spring and summer seasons, approximately from May to September, and the local spring is a very short season, the $\delta^{13}C$ value of the plants mainly reflects the summer precipitation variability. Finally, plant cellulose is highly resistant to decomposition. Both cellulose and its isotopes are highly stable over periods of approximately 10^5 years[6]. Therefore, the $\delta^{13}C$ value of the peat plants' cellulose can be considered a good indicator of the variability of summer rainfall[6,21,23]. We sampled the peat core specimens at intervals of 1 cm and extracted cellulose from the vegetation residues of each specimen using a sodium chlorite oxidation method[6,21,23]. The composition of the stable carbon isotopes of the cellulose specimen was measured and expressed as $\delta^{13}C = [(^{13}C/^{12}C)_{sample}/(^{13}C/^{12}C)_{standard}] - 1$. The lower (or more negative) the $\delta^{13}C$ value is, the greater the summer rainfall, and vice versa[6,21,23].

Table 2 | Radiocarbon dates of the Chaiwobu peat profile

				Calibrated age ranges (yr BP)	Calibrated age	
Lab no.	Depth (cm)	$\delta^{13}C$ (‰,VPDB)	^{14}C age (yr BP)	1σ	(yr BP)	(yr AD)
XC-30	30	−25.17	106 ± 28	−2–256	112	1839
XC-38	38	−24.92	200 ± 30	−1–292	179	1772
XC-48	48	−25.11	540 ± 30	524–621	547	1404
XC-55	55	−25.51	1123 ± 29	980–1058	1020	931
XC-60	60	−26.17	1220 ± 30	1080–1221	1147	
XC-70	70	−25.30	1831 ± 31	1733–1815	1770	
XC-80	80	−24.89	1874 ± 30	1741–1871	1821	
XC-100	100	−25.43	2480 ± 30	2488–2705	2575	
XC-130	130	−25.02	2719 ± 31	2781–2845	2815	
XC-142	142	−25.64	2900 ± 30	2973–3075	3037	
XC-143	143	−25.72	3010 ± 32	3160–3319	3219	
XC-146	146	−25.47	3670 ± 30	3929–4080	4005	
XC-149	149	−25.22	3840 ± 30	4156–4339	4249	
XC-152	152	−24.93	5360 ± 30	6027–6267	6148	
XC-170	170	−24.71	6220 ± 30	7025–7237	7144	
XC-185	185	−24.60	6429 ± 38	7323–7417	7361	
XC-200	200	−24.75	6989 ± 38	7765–7923	7826	
XC-220	220	−24.79	7362 ± 40	8054–8295	8180	
XC-259	259	−24.87	7760 ± 41	8465–8592	8538	

^{14}C dating and the time resolution for the Chaiwobu peat profile. To build the ^{14}C dating timescale, we first described the properties of the peat column samples collected at the field sampling location and subdivided the column samples into several small fractions according to the colour and texture changes of the fresh peat samples. The colour and texture of each small fraction were the same; thus, the sedimentary environment and the accumulation speed of each small fraction have been considered to be the same. Then, we set up a ^{14}C age control point at the junction of two small column samples and added several ^{14}C age control points in the fraction from the recent millennium and in some thicker small fractions on the column sample. A total of 19 ^{14}C age control points were established (Fig. 6 and Table 2). The peat cellulose samples of the control point were prepared for graphite targets and their ^{14}C intensity was determined in the AMS Laboratory of the National Institute for Environmental Studies in Tsukuba, Japan to obtain the ^{14}C age[57]; the chronological age was determined after correction using the CALIB-6.1 programme[58]. We then obtained the chronological age sequence of the ^{14}C from the Chaiwobu peat profile via linear interpolation. The Chaiwobu peat core sample was cut continuously into 1-cm subsamples equivalent to a mean time resolution of approximately 33 years. The mean sedimentation rate in the entire Chaiwobu peat profile was approximately 31 cm per 1000 years, which is sufficient to resolve the millennial-scale variability. In the recent millennium, four ^{14}C age control points were established (Fig. 6 and Table 2), and the sedimentation rate reached 2.6 cm per 50 years or 5 cm per 100 years, allowing us to discuss the rainfall variation on decadal to centennial timescales.

1. Yang, X. P. *et al.* Quaternary environmental changes in the drylands of China – A critical review. *Quatern. Sci. Rev.* **30**, 3219–3233 (2011).
2. Winkler, M. G. & Wang, P. K. *Global Climates since the last glacial maximum,* Wright, H. E. *et al.* (eds.), 221–261 (Univ. of Minnesota Press, MN, 1993).
3. Rhodes, T. E. *et al.* A Late Pleistocene-Holocene lacustrine record from Lake Manas, Zunggar (northern Xinjiang, western China). *Palaeogeogr. Palaeoclimatol. Palaeoecol.* **120**, 105–121 (1996).
4. Shi, Y. F. *et al.* Recent and future climate change in northwest China. *Clim. Change* **80**, 379–393 (2007).
5. Tarasov, P. *et al.* Satellite- and pollen-based quantitative woody cover reconstructions for northern Asia: Verification and application to late-Quaternary pollen data. *Earth Planet Sci. Lett.* **264**, 284–298 (2007).
6. Hong, B. *et al.* Anti-phase oscillation of Asian monsoons during the Younger Dryas period: Evidence from peat cellulose δ^{13}C of Hani, Northeast China. *Palaeogeogr. Palaeoclimatol. Palaeoecol.* **297**, 214–222 (2010).
7. An, Z. S. *et al.* Interplay between the Westerlies and Asian monsoon recorded in Lake Qinghai sediments since 32 ka. *Sci. Rep.* **2**, 619 DOI: 10.1038/srep00619 (2012).
8. Zhang, J. B. & Deng, Z. F. *An introduction to precipitation in the Xinjiang Autonomous Region.* 132–156, (Meteorological Press, Beijing, 1987).
9. Yin, X. L. *et al.* Hydro-chemical and isotopic research in Chaiwobu basin, Urumqi river catchment. *Acta Geologica Sinica* **84**, 439–448 (2010).
10. Gao, Y. X., Xu, S. Y. & Guo, Q. Y. *Some problems of East Asian monsoon.* Gao, Y. X. & Xu, S. Y., (eds.), 49–63 (Science Press, Beijing, 1962).
11. Wang, B., Clemens, S. C. & Liu, P. Contrasting the Indian and East Asian monsoons: implications on geologic timescales. *Marine Geology* **201**, 5–21 (2003).
12. Morrill, C., Overpeck, J. T. & Cole, J. E. A synthesis of abrupt changes in the Asian summer monsoon since the last deglaciation. *Holocene* **13**, 465–476 (2003).
13. Blyakharchuk, T. A., Wright, H. E., Borodavko, P. S., van der Knaap, W. O. & Ammann, B. Late Glacial and Holocene vegetational history of the Altai Mountains (southwestern Tuva Republic, Siberia). *Palaeogeogr. Palaeoclimatol. Palaeoecol.* **245**, 518–534 (2007).
14. Rudaya, N. *et al.* Holocene environments and climate in the Mongolian Altai reconstructed from the Hoton-Nur pollen and diatom records: a step towards better understanding climate dynamics in Central Asia. *Quat. Sci. Rev.* **28**, 540–554 (2009).
15. Chen, F. H. *et al.* Holocene moisture evolution in arid central Asia and its out-of-phase relationship with Asian monsoon history. *Quat. Sci. Rev.* **27**, 351–364 (2008).
16. Liu, X. Q. *et al.* Evolution of Chaka Salt Lake in NW China in response to climatic change during the Latest Pleistocene–Holocene. *Quat. Sci. Rev.* **27**, 867–879 (2008).
17. Li, X. Q., Zhao, K. L., Dodson, J. & Zhou, X. Y. Moisture dynamics in central Asia for the last 15 kyr: new evidence from Yili Valley, Xinjiang, NW China. *Quat. Sci. Rev.* **30**, 3457–3466 (2011).
18. Friedli, H., Lötscher, H., Oeschger, H., Siegenthaler, U. & Stauffer, B. Ice core record of the 13C/12C ratio of atmospheric CO_2 in the past two centuries. *Nature* **324**, 237–238 (1986).
19. Indermühle, A. *et al.* Holocene carbon-cycle dynamics based on CO_2 trapped in ice at Taylor Dome, Antarctica. *Nature* **398**, 121–126 (1999).
20. Fleitmann, D. *et al.* Holocene forcing of the Indian monsoon recorded in a stalagmite from southern Oman. *Science* **300**, 1737–1739 (2003).
21. Hong, Y. T. *et al.* Correlation between Indian Ocean summer monsoon and North Atlantic climate during the Holocene. *Earth Planet Sci. Lett.* **211**, 371–380 (2003).
22. Gupta, A. K., Das, M. & Anderson, D. M. Solar influence on the Indian summer monsoon during the Holocene. *Geophys. Res. Lett.* **32**, 1–4 (2005).
23. Hong, Y. T. *et al.* Inverse phase oscillations between the East Asian and Indian Ocean summer monsoons during the last 12000 years and paleo-El Niño. *Earth Planet Sci. Lett.* **231**, 337–346 (2005).
24. Ran, M. & Feng, Z. Holocene moisture variations across China and driving mechanisms: A synthesis of climatic records. *Quatern. Int.* **313–314**, 179–193 (2013).
25. Zhou, T. J. & Yu, R. C. Atmospheric water vapor transport associated with typical anomalous summer rainfall patterns in China. *J. Geophys. Res.* **110**, D08104, doi:10.1029/2004JD005413 (2005).
26. Wang, H. J. & Chen, H. P. Climate control for southeastern China moisture and precipitation: Indian or East Asian monsoon? *J. Geophys. Res.* **117**, D12109, doi:10.1029/2012JD017734 (2012).
27. Bond, G. *et al.* A Pervasive millennial-scale cycle in North Atlantic Holocene and glacial climates. *Science* **278**, 1257–1266 (1997).
28. Gupta, A. K., Anderson, D. M. & Overpeck, J. T. Abrupt changes in the Asian southwest monsoon during the Holocene and their links to the North Atlantic Ocean. *Nature* **421**, 354–357 (2003).
29. Hong, Y. T. *et al.* Synchronous climate anomalies in the western North Pacific and North Atlantic regions during the last 14,000 years. *Quatern. Sci. Rev.* **28**, 840–849 (2009).
30. Wanner, H., Solomina, O., Grosjean, M., Ritz, S. P. & Jetel, M. Structure and origin of Holocene cold events. *Quatern. Sci. Rev.* **30**, 3109–3123 (2011).
31. Lawler, A. Bridging East and West. *Science* **325**, 940–943 (2009).
32. Ahn, Jinho *et al.* Atmospheric CO_2 over the last 1000 years: A high-resolution record from the West Antarctic Ice Sheet (WAIS) Divide ice core. *Global Biogeochem. Cy.* **26**, GB2027, doi:10.1029/2011GB004247 (2012).
33. Schelske, C. L. & Hodell, D. A. Using carbon isotopes of bulk sedimentary organic matter to reconstruct the history of nutrient loading and eutrophication in Lake Erie. *Limnol. Oceanogr.* **40**, 918–929 (1995).
34. Yuan, Y., Li, J. & Zhang, J. 380 years precipitation reconstruction from tree rings for the north slope of the Middle Tianshan Mountains. *Acta Meteorologica Sinica* **15**, 95–104 (2001).
35. Dai, A. Increasing drought under global warming in observations and models. *Nature Clim. Change* **3**, 52–58 (2013).
36. Wang, Y. *et al.* The Holocene Asian monsoon: links to solar changes and North Atlantic climate. *Science* **308**, 854–857 (2005).
37. Fleitmann, D. *et al.* Holocene ITCZ and Indian monsoon dynamics recorded in stalagmites from Oman and Yemen (Socotra). *Quat. Sci. Rev.* **26**, 170–188 (2007).
38. Shukla, J. & Paolina, D. The Southern Oscillation and long range forecasting of the summer monsoon rainfall over India. *Monthly Weather Review* **111**, 1830–1837 (1983).
39. Webster, P. J. & Fasullo, J. *Encyclopedia of Atmospheric Sciences,* Holton, J. & Curry, J. A. (eds.), 1370–1386 (Academic Press, London, 2003).
40. Kumar, K. K., Rajagopalan, B., Hoerling, M., Bates, G. & Cane, M. Unraveling the mystery of Indian monsoon failure during El Niño. *Science* **314**, 115–119 (2006).
41. Meehl, G. A. & Hu, A. Megadroughts in the Indian monsoon region and southwest North America and a mechanism for associated multidecadal pacific sea temperature anomalies. *J. Climate* **19**, 1605–1623 (2006).
42. Sun, S. Q. & Ying, M. Subtropical high anomalies over the Western Pacific and its relations to the Asian monsoon and SST anomaly. *Adv. Atmos. Sci.* **16**, 559–568 (1999).
43. Ying, M. & Sun, S. Q. A study on the response of subtropical high over the western Pacific on the SST anomaly. *Chin. J. Atmos. Sci.* **24**, 193–206 (2000).
44. Wu, G. X., Chou, J. F., Liu, Y. M., Zhang, Q. Y. & Sun, S. Q. Review and prospect of the study on the subtropical anticyclone. *Chin. J. Atmos. Sci.* **27**, 503–517 (2003).
45. Koutavas, A., Lynch-Stieglitz, J., Marchitto, T. M. & Sachs, J. P. El Niño-like pattern in Ice Age tropical Pacific sea surface temperature. *Science* **297**, 226–230 (2002).
46. Koutavas, A, deMenocal, P. B., Olive, G. C. & Lynch-Stieglita, J. Mid-Holocene El Niño-Southern Oscillation (ENSO) attenuation revealed by individual foraminifera in eastern tropical Pacific sediments. *Geology* **34**, 993–996 (2006).
47. Chen, G. S., Liu, Z., Clemens, S. C., Prell, W. L. & Liu, X. D. Modeling the time-dependent response of the Asian summer monsoon to obliquity forcing in a coupled GCM: a PHASEMAP sensitivity experiment. *Clim. Dynam.* **36**, 695–710 (2011).
48. Wang, Y., Jian, Z. M. & Zhao, P. Extratropical modulation on Asian summer monsoon at precessional bands. *Geophys. Res. Lett.* **39**, L14803, doi:10.1029/2012GL052553 (2012).
49. Bengtsson, L. The global atmospheric water cycle. *Environ. Res. Lett.* **5**, 1–8 (2010)
50. Clark, P. U. *et al.* Global climate evolution during the last deglaciation. *P. Natl. Acad. Sci. USA* **109**, E1134–E1142 (2012).
51. Wang, Y. J. *et al.* A high-resolute absolute-dated Late Pleistocene monsoon record from Hulu Cave, China. *Science* **294**, 2345–2348 (2001).
52. Dykoski, C. A. *et al.* A high-resolution absolute-dated Holocene and deglacial Asian monsoon record from Dongge Cave, China. *Earth Planet Sci. Lett.* **233**, 71–86 (2005).
53. Zhou, W., Zheng, Y., Meyers, P. A., Timothy Jull, A. J. & Xie, S. Postglacial climate-change record in biomarker lipid compositions of the Hani peat sequence, Northeastern China. *Earth Planet Sci. Lett.* **294**, 37–46 (2010).
54. Delgado-Baquerizo, M. *et al.* Decoupling of soil nutrient cycles as a function of aridity in global drylands. *Nature* **502**, 672–679 (2013).
55. Francey, R. J. & Farquhar, G. D. An explanation of ^{13}C/^{12}C variations in tree rings. *Nature* **297**, 28–31 (1982).
56. Schleser, G. H. *Paläoklimaforschung*, Frenzel, B. *et al.* (eds.), 71–96 (Strasbourg, France, 1995).

57. Uchida, M. *et al.* Radiocarbon-based carbon source quantification of anomalous isotopic foraminifera in last glacial sediments in the western North Pacific. *Geochem. Geophys. Geosyst.* **9**, Q04N14, doi: 10.1029/2006GC001558 (2008).
58. Reimer, P. J. *et al.* IntCal09 and Marine09 radiocarbon age calibration curves, 0–50,000 years cal BP. *Radiocarbon* **51**, 1111–1150 (2009).
59. Mann, M. Climate over the past two millennia. *Annu. Rev. Earth Planet. Sci.* **35**, 111–136 (2007).
60. Moy, C. M., Seltzer, G. O., Rodbell, D. T. & Anderson, D. M. Variability of El Niño/Southern Oscillation activity at millennial timescales during the Holocene epoch. *Nature* **420**, 62–165 (2002).

Acknowledgments

This work was funded by the National Natural Science Foundation of China (Grant No. 41173127, 41373134).

Author contributions

B.H. and Y.H. designed this study. Drilling and sampling were done by B.H., Y.H., X.L., Y.Z. and Y.W. Laboratory analyses were done by M.U., Y.S., B.H., Y.Z., N.A. and Y.W. The plant residues in peat were identified by X.L. Data analysis and palaeoclimatic interpretations were done by B.H., F.G. and Y.H. The paper was written by B.H., F.G. and Y.H. All authors reviewed the manuscript. Y.H. coordinated the research project.

Additional information

Supplementary information accompanies this paper at http://www.nature.com/scientificreports

Competing financial interests: The authors declare no competing financial interests.

How to cite this article: Hong, B. *et al.* Increasing summer rainfall in arid eastern-Central Asia over the past 8500 years. *Sci. Rep.* **4**, 5279; DOI:10.1038/srep05279 (2014).